ELSEVIER

Ultrasonic wave dispersion and attenuation in fresh mortar

D.G. Aggelis[a,b], T.P. Philippidis[a,b],*

[a]*Department of Mechanical Engineering and Aeronautics, University of Patras, P.O. Box 1401, Panepistimioupolis, Rion, Patras 26504, Greece*
[b]*Institute of Chemical Engineering and High Temperature Chemical Processes (FORTH/ICE-HT), Patras 26500, Greece*

Abstract

Results from an experimental study of ultrasonic, through-transmission, wave propagation on fresh cementitious material are discussed in this paper. The propagation characteristics of different frequency tone-bursts revealed the strong dispersive behavior of this type of materials while using sine-sweep excitation, the attenuation up to about 1 MHz was examined. Sand content and size exercise significant influence on wave parameters while entrapped air bubbles seem to dominate the attenuation at low frequencies since cement paste specimens, containing no sand, exhibit strong attenuation. The possibility of mortar composition characterization within 10 min after mixing is also addressed leading to encouraging results.
© 2004 Elsevier Ltd. All rights reserved.

Keywords: Fresh concrete; Ultrasound; Velocity; Dispersion; Attenuation

1. Introduction

Concrete, the most widely used construction material exhibits properties developing with time. Immediately after mixing, it behaves as a liquid suspension of various particles (cement grains, aggregates, air bubbles) in water while as the hydration reaction proceeds it is transformed into a rigid porous material with considerable load bearing capacity. To achieve the required mechanical properties careful design and mixing of the constituent materials must take place. These properties and mainly the compressive strength are usually examined through the compressive test 28 days after placement on specimens sampled from the fresh material and cured in proper conditions. However, it would be ideal to predict the final strength at early ages, even before the material is placed in the forms [1]. Ensuring that all standard procedures are followed and that concrete is batched according to the selected mixture proportions, it is not likely that the properties of the hardened material will be other than satisfactory [2]. Therefore, quality characterization of concrete, while it is still in the fresh state, is highly desirable.

The most crucial parameter affecting strength and durability of concrete is considered to be the water dosage or the water to cement ratio by mass, *w/c*, being inversely related to strength [3]. Although for any given application a concrete with a proper *w/c* can be designed, there is no guarantee that the same concrete will be produced. This can be due to incorrect weighting, absorption of a portion of water in the porosity of not properly hydrated aggregates or deliberate addition of water to make concrete more workable [3]. The usefulness of quality estimation of fresh concrete through composition control and especially *w/c* determination has been stated in a number of recent works [1,3–9], while also a wide variety of approaches have been followed towards this aim. However, all above approaches suffer from inherent difficulties such as the severely attenuative nature of fresh concrete [1], the variability in aggregate content and type [4–6] or the presence of chemical admixtures [4]. Other methods are extremely sensitive to small measurement inaccuracies, complicated or time-consuming [6,8]. Apart from these, the data population in above works cannot always be considered adequate for reliable determination of *w/c* ratio. Therefore, so far there is no generally accepted and applicable method for quality prediction of hardened concrete when it is still in the fresh state.

As stress wave propagation is concerned, it has qualitatively been shown that material with lower *w/c* ratio exhibits

higher wave velocity and waveform energy in the hardened [10] or fresh state [7,11–17] without, however, adequate information concerning the possibility of *w/c* accurate determination, since generally the above studies were focused on the monitoring of the hydration process under different conditions. Additionally, measurements are not conducted for at least 15 min after mixing or even more, with the exception of Ref. [15], while the difference in *w/c* ratio seems to have a more clear influence on the wave velocity after the first few hours.

Nevertheless, the inhomogeneous nature of fresh concrete consisting of cement and sand grains, coarse aggregates and even air bubbles suspended in water makes the characterization of the material a quite complicated task. The understanding of the interaction of ultrasound with the several phases co-existing in the suspension is a first necessary step in order to correctly interpret stress wave propagation data.

In the present paper, experimental results concerning frequency dependence of wave velocity and attenuation in fresh mortar are described. Using either tone-burst excitation signals or broad band ones in the form of sine-sweep, a systematic study of wave propagation in such a suspension is performed, revealing the influence of the different mix design parameters as the sand content, grain size and *w/c*. The material, as typically expected for any particle suspension in fluid [18] exhibits dispersive behavior, while the high level of attenuation attributed to a number of different processes inhomogeneity induces [19], restricts the used wavepath to the order of 10 mm.

Although numerous studies concerning wave propagation in various systems of suspensions have been published, no systematic study on the specific influence of fresh concrete mix design parameters in wave dispersion and attenuation has seen publicity so far, to the authors' knowledge. Exploiting the relation between wave characteristics and mix design parameters, the possibility of fresh mortar composition characterization is addressed.

This study is a follow-up of a national research project aiming at the quality characterization of concrete through composition control. Results as to *w/c* determination of hardened concrete were quite successful [20], while the study now is concentrated on the examination of fresh material. Using an appropriate combination of wave generator board and ultrasonic transducers, the possibilities of enhancing NDT results by dispersion and attenuation parameters, obtained for a wide band of frequencies is examined.

2. Experimental procedure

The experimental set-up consists of a Physical Acoustics Corporation (PAC) waveform generator WaveGen 1410, two broadband Panametrics V413 transducers of 500 kHz center frequency, PAC preamplifier 1220A and a PAC Mistras 2001 acoustic emission data acquisition system. The rectangular sensors are mounted in plexi-glass plates facing each other, while a U-shaped rubber plate is placed in between defining the volume to be occupied by the specimen, Fig. 1. The thickness of the rubber pad is 10.6 mm and the device is secured by the use of screws. This thickness was selected since lower values would cause problems concerning the workability of sand rich mortar while higher distances between sensors, up to 25 mm, that have been used, revealed that certain bands of frequencies do not survive and more specifically below 150 and above 500 kHz.

The waveforms selected as electric input to the transducer is of the shape of Fig. 2(a). This sinusoidal wave in sinusoidal envelope introduces a relatively narrow band excitation to the sensor, as can be seen in Fig. 2(b) where the Fourier transform of the above signal is depicted. Several (30) similar tone-burst signals with central frequencies from 20 kHz up to about 1 MHz at certain intervals are applied consequentially to each specimen. Due to severe attenuation, in most cases reliable signals were acquired up to 800 kHz. The use of broadband excitation has also been adopted through the introduction of sine-sweep pulses, as seen in Fig. 2(c). This way the electric signal exhibits approximately constant magnitude throughout the first megahertz as seen in Fig. 2(d) and depending of course on the sensor's response a wide range of frequencies enter the material.

Indeed, since the specific transducer exhibits a maximum sensitivity around 500 kHz, it was deemed necessary to test its response throughout the whole band of frequencies used in a face to face configuration with a thin layer of grease between the sensor faces serving as couplant. As seen in Fig. 3, pulses with frequencies away from the high sensitivity range of the transducer are well transmitted without serious distortion or alteration of frequency content even for the cases of 20 kHz, Fig. 3(a) and (b) and 800 kHz, Fig. 3(c) and (d), the only difference lying on the amplitude axis, behavior which does not influence wave velocity measurements. Concerning sine-sweep excitation, Fig. 4(a) and (b) depict the time and frequency face to face responses, respectively, showing that frequencies within the band 20–800 kHz are presented into the material. The sensor preference is obvious; however, this effect is cancelled in attenuation measurements since the water specimen waveforms used as reference are obtained with the same sensors. Nevertheless, as will be mentioned later, another pair of transducers was used to obtain attenuation spectra for some indicative cases. Specifically Panametrics V133 of center frequency 2.25 MHz were used showing similar spectra. It should be noted that the length of each collected waveform was 15,360 points, with a sampling rate of 10 MHz.

One specimen was tested from each composition as seen in Table 1. Mortar containing various sand contents by volume, *s*, from 0%, which is simply cement paste, up to even 47.5% and different *w/c* in a range widely used in practice was produced and tested. In total, about 80
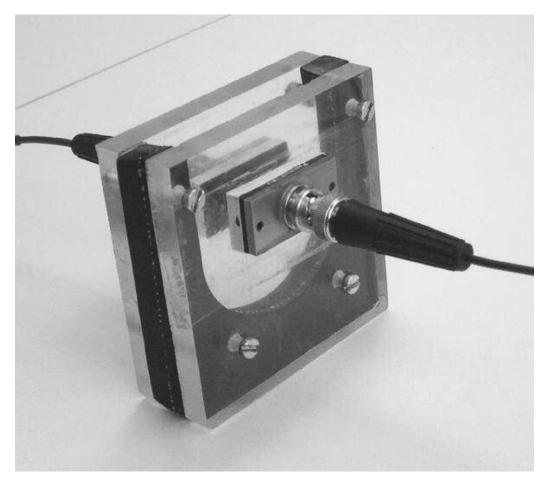
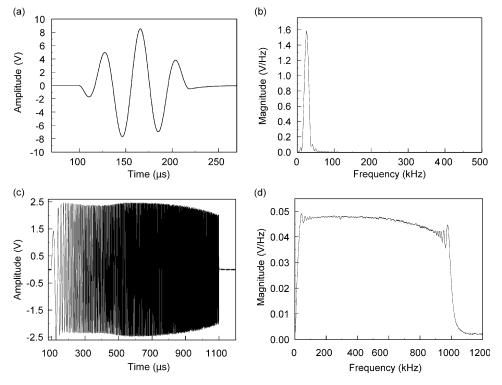Fig. 1. Fresh mortar container and ultrasonic sensors.

Fig. 2. Input electric signal of three cycles at 25 kHz in sinusoidal envelope in time domain (a) and in frequency domain (b), 10 kHz–1 MHz sine-sweep electric signal in time domain (c) and in frequency domain (d).
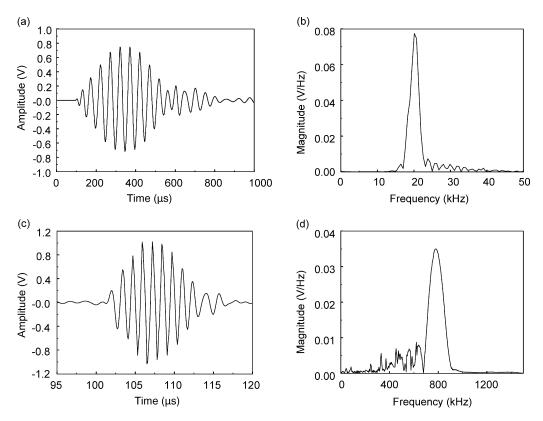
Fig. 3. Face to face sensor response in input of 20 kHz in time (a) and frequency domain (b) and in input of 800 kHz in time (c) and frequency domain (d).

specimens were tested. However, signals obtained by compositions with *s* greater than 40% are not employed in the analysis since these specimens exhibited workability problems, considering the small size of the container.

The ingredients (cement II 32.5, limestone sand and water) were weighted with 0.1 mg accuracy, mixed and stirred for 5 min. Then, the material was poured between the sensors and compacted by means of a stick, which resulted in
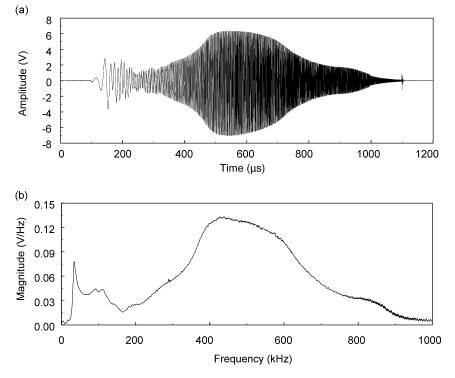

Fig. 4. Face to face sensor response in sine-sweep input in time (a) and frequency domain (b).

Table 1
Mix parameters of tested specimens

w/c	s (%)												
	0 (paste)	10	20	25	27.5	30	32.5	35	37.5	40	42.5	45	47.5
0.45	X	X	X	X	X	X	X	X	X	X			
0.475						X	X	X	X	X			
0.49					X	X	X	X	X	X			
0.50	X	X	X	X	X	X	X	X	X	X			
0.51						X	X	X	X	X	X		
0.525	X		X		X	X	X	X	X	X	X	X	
0.54		X		X	X	X	X	X	X	X			
0.55	X +	X	X	X	X	X +	X	X	X*	X**	X	X	X

X denotes manufactured and tested compositions. Composition repeated with (*) three different sand sizes, (**) two different sand sizes and (+) different sensor.

the release of visible air bubbles on the surface. Therefore, the measurements start approximately 7 min after mixing of the ingredients.

3. Dispersion

As stated above, the acquisition system is dedicated to acoustic emission applications providing real time analysis and feature extraction of waveforms in time and frequency domain. However, leading both the electric signal from the wave generator and the received signal from the transducer to separate, synchronized channels, the value of pulse velocity through the material can be obtained from the time shift between the waveforms acquired by the two channels, excluding sensor delay times, a procedure that will be explained below. The onset of each signal was set as the first threshold crossing. In order to evaluate the noise level, a pre-trigger time of 100 μs was recorded before each signal. The threshold was set equal to the maximum amplitude exhibited in this period.

It is essential for such measurements that noise level does not mask the first disturbance arrival. In Fig. 5, an example is given of how noise and threshold values affect pulse velocity readings. Fig. 5(a) depicts a 175 kHz waveform of mortar with $w/c = 0.525$ and $s = 35\%$ in time domain. Fig. 5(b) brings into focus the first 115 μs of this waveform, showing also the threshold line, set equal to the maximum
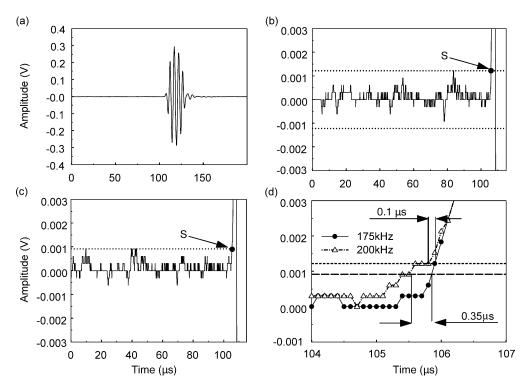

Fig. 5. Waveform of 175 kHz through mortar (a), the first 115 μs of the same waveform (b), of a waveform of 200 kHz (c) and the effect of threshold value on selection of starting point.

noise amplitude (1.221 mV). Based on this pattern, arrival time corresponds to point S. However, due to its randomness, noise exhibits slight fluctuations as can be seen in Fig. 5(c) where a waveform of 200 kHz on the same specimen is shown. Threshold in this case is 0.916 mV. This small difference in measured noise affects the velocity measurement up to a small degree as can be seen in Fig. 5(d). This figure contains the critical microseconds where the signal undoubtfully rises for both cases of (b) and (c). Applying the two different thresholds, the onsets of the two signals, are 0.35 μs (using linear interpolation for the 175 kHz case) or 0.1 μs apart, leading to differences of 169 and 26 m/s in the measured pulse velocity. This example shows the reason for the observed experimental scatter that is evident in following sections. Although acute discrepancies in transit time of pulses with neighboring central frequencies are not likely, in the specific example, it is a certain fact that the waveform of 200 kHz, as revealed by Fig. 5(d), rises earlier than that of 175 kHz, fact that is securely measured by the threshold crossing algorithm. Indeed, the application of such a simple noise-dependent threshold algorithm, built in Visual Basic, was the more suitable and time-effective solution for the treatment of the numerous waveforms with the aid of eye assistance being necessary only in a few extreme cases of higher noise value. It is important to mention that generally, the noise level of the specific set-up is quite small, allowing feature extraction without application of filters or other techniques to enhance the signal to noise ratio.

3.1. Discussion on accuracy of velocity measurements

The main source of error in such measurements is the system time delay, which exercises a significant influence as will be seen. This behavior is attributed to the propagation of the wave through the sensor's wearplate as well as any electronic switching time or cable delays and should be taken into account for enhanced accuracy [21]. Indeed, in the specific case of the reduced wavepath, due to mortar attenuation, transit times are also small, making the compensation for sensor delays mandatory for realistic velocity measurement. In order to determine the delay time, δt, measurements were conducted in reference media. The distance between the sensors was set to different values for each measurement. However, since the velocity of the reference medium, C_{ref}, is constant regardless of the wavepath, δt can be calculated as follows. For two different configurations (wavepaths S_1 and S_2) and any specific pulse, the time difference between the introduction of the electric signal and the arrival of the received was measured, t_1 and t_2, respectively. These values contain the delay δt :

$$\delta t = \frac{S_2 t_1 - S_1 t_2}{S_2 - S_1} \tag{1}$$

To improve accuracy, the delay was measured using different media namely water, fresh cement paste, a steel calibration block and concrete specimens of different sizes. The results were quite close, while not exhibiting any noticeable dependence on the central frequency of the tone-burst. Therefore, the delay was calculated as the average of the delay exhibited in all different calibration measurements, namely 1.575 μs. This value was subtracted thereafter from the time shift between the received and the electric input signal. Indicatively, it should be mentioned that using the value of $\delta t = 1.575$ μs the water sound velocity calculated from all different tone-bursts results in an almost constant value of 1501 m/s regardless of the frequency with a standard deviation of 7.8 m/s. The necessity of taking delay time into account can be easily seen, since, for example, for the pulse of 500 kHz, concerning a cement paste specimen ($w/c = 0.50$), the transit time is calculated 6.52 μs while, without the system delay correction, it is measured 8.09 μs. Therefore, the velocity (1580 m/s) without considering the delay effect would be underestimated to 1275 m/s, which is approximately 19% lower. For mortar specimens with high sand content, since the transit time is lower (approximately 4 μs), as will be seen in Section 3.2, ignoring the delay would cause even greater discrepancies (more than 25% underestimation of pulse velocity). Although neglecting the time delay does not prevent from comparing between different materials' transit times, it is essential for realistic pulse velocity measurement.

3.2. Sand content effect

In Fig. 6 the velocity vs frequency curve of material with different sand contents s, is depicted. In both cases of Fig. 6, the cement paste follows a smooth curve starting at around 1500 m/s, climbing to approximately 1600 m/s at about 100 kHz and staying approximately constant for higher frequencies. The addition of sand, up to 30 or 35% by volume, increases the values of velocities throughout all bands examined since the sand richest mix exhibits the highest velocity values for both cases. It is also seen that the increase of sand content shifts the maximum of the velocity curve to higher frequencies. However, velocity of mortar specimens has the tendency to decrease for the last high frequencies examined. Thus, it seems that aggregates have a significant impact in velocity influencing both the elevation of the curve as well as the increasing rate for low frequencies. Velocities higher than water generally were expected since the addition of cement and sand grains in water reduces the effective compressibility resulting in higher sound velocity. It is noted that besides the symbols, which are the calculated values of velocity by means of the threshold crossing algorithm, curves fitting the data are also drawn for clarity in Fig. 6(a) and (b), since the experimental scatter in many cases is confusing. In contrast to mortar, paste velocity curves seem to exhibit only slight increase for the first 150 kHz. Bearing in mind that the size of cement grains is of the order of 50 μm, several orders of magnitude
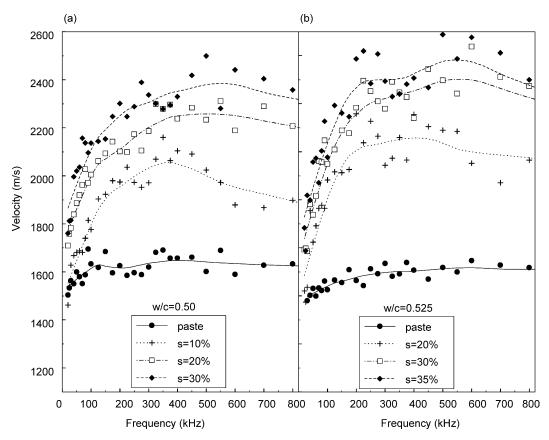
Fig. 6. Effect of sand content on dispersion curves of (a) *w/c* = 0.50 and (b) *w/c* = 0.525 specimens.

lower than the applied wavelengths, cement paste should be expected to exhibit the behavior of a homogeneous liquid. However, and since no sand grains are present, it follows that the observed weak dispersion should be attributed to other sources of inhomogeneity. Indeed, no matter how sufficient the compaction may be, there is always an entrapped air void content that generally falls between 1 and 10% by volume for insufficient compaction. The addition of sand grains increases even more the inhomogeneity level influencing the smooth curve of paste velocity vs frequency.

3.3. Water content effect

The hydration reaction between water and cement grains essentially starts after a 'dormant' period of some hours. This has been manifested in various works [11–16] where the ultrasonic parameters used to monitor hydration seem to undergo change after a period of some hours after mixing of the ingredients while certainly for the first minutes there is no detectable modification. Therefore, for the first minutes, the *w/c* of fresh mortar affects mainly the density of the medium since low *w/c* means higher density and vice versa. Variation in this parameter seems to have a slight influence on the dispersion curve as can be seen in Fig. 7. Sand content for all specimens of Fig. 7(a) is 30% and of Fig. 7(b) is 35% while only the *w/c* of the paste varies. It seems that water content has a smaller impact on pulse velocity for

fresh material compared to the influence of sand content on velocity. It is concluded that for materials with the same sand content, low *w/c* specimens exhibit higher pulse velocities for most frequencies, Fig. 7(a), without, however, clear and repeatable discrepancies that could lead to reliable conclusions, Fig. 7(b).

4. Attenuation

Wave propagation in such systems is so complicated as is the task to quantify the contributions of different mechanisms to the total attenuation. Generally, the most important mechanisms of attenuation in a suspension are: absorption losses in each of the individual phases, visco-inertial losses due to density discrepancies of the constituent materials, thermal dissipation losses and scattering [22].

In the present study, total attenuation was calculated using the spectra of the sine-sweep pulses through the examination material. These spectra were normalized with a point-by-point division with the reference spectrum, which in this case comes from a water specimen

$$\alpha(f) = -\frac{20}{x}\log\left(\frac{A(f)}{A_{\mathrm{w}}(f)}\right) \qquad (2)$$

where $\alpha(f)$ is the attenuation coefficient with respect to frequency, x is the distance between the sensors (10.6 mm),
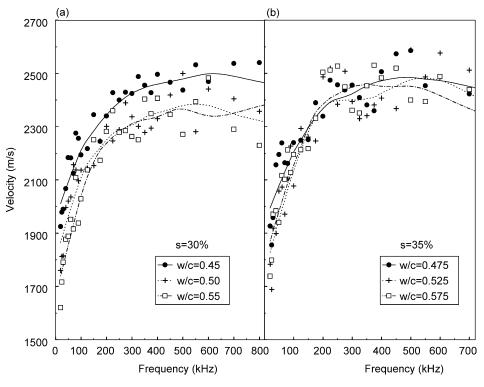
Fig. 7. Effect of *w/c* ratio on dispersion curves of (a) *s* = 30% and (b) *s* = 35% specimens.

A(f) and *A*$_w$(*f*) are the spectra of the liquid suspension and water, respectively. The sampling rate of 10 MHz is adequate for the digitization of even the last part of the sine-sweep signal containing frequencies up to 1 MHz. Therefore, the digitized waveform can be reliably used for determination of frequency content of the wave propagating through the material and the attenuation of each frequency.

4.1. Sand effect

Measurements conducted in mortars containing different amounts of sand revealed the pronounced effect of sand content in the overall attenuation. In Fig. 8(a), the attenuation vs frequency curves for four different sand content specimens, sharing though the same *w/c* of 0.50 are
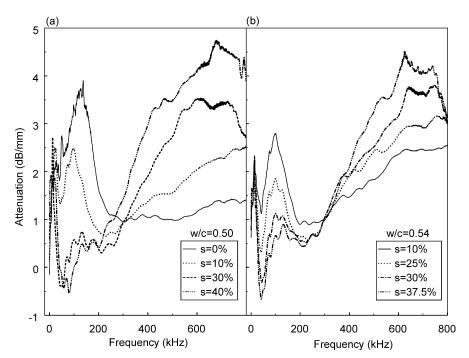

Fig. 8. Effect of sand content on attenuation vs frequency curves of (a) *w/c* = 0.50 and (b) *w/c* = 0.54 specimens.
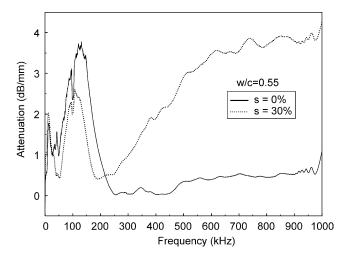
Fig. 9. Effect of sand content on attenuation vs frequency curves obtained with sensor V133.

depicted. Concerning the paste specimen ($s = 0\%$), a certain attenuation is observed for frequencies lower than 300 kHz, while afterwards attenuation decreases and stays approximately constant up to the highest frequency tested. The addition of sand decreases the low frequency attenuation, while for a range of frequencies below 100 kHz, mortars with s equal or more than 30% exhibit amplitudes higher than the water specimen (negative attenuation). Attenuation values of all different materials seem comparable around 300 kHz while for higher frequencies they increase accordingly to s values. The same trend is depicted in Fig. 8(b) for different sand

contents in a host medium of $w/c = 0.54$. Here the coincidence of attenuation of different specimens for frequencies around 300 kHz is even more pronounced. This behavior, however, is imposed by the material itself. In order to exclude the possibility of sensor performance masking the calculated attenuation, the V133 sensor was also used and responses to sine-sweep signals were obtained for indicative cases of water, paste and mortar. As seen in Fig. 9, the attenuation of paste and mortar follows the same trend as in Fig. 8, while the curves cross at a point above 200 kHz, showing that the sensor contribution to the measured attenuation curves is not so important.

Therefore, the commonly met trend of increasing attenuation with inclusion content in suspensions is also observed in this study for frequencies above 200 kHz. It is more likely the manifestation of scattering mechanisms that start to dominate wave propagation at high frequencies resulting in the high attenuation values observed for sand rich mixes. The behavior at low frequencies, however, shows an opposite trend, which could be assumed to be due to the air bubbles entrapped in mortar, the presence of which has been reported to play an essential role in the macroscopic behavior [16].

The tendencies shown in Fig. 8 concerning low and high frequency attenuation are depicted more clearly in Fig. 10. Fig. 10(a) contains two examples of attenuation vs sand content, s for low frequencies, 80 and 90 kHz, where the decreasing trend is obvious. However, for frequencies higher than 300 kHz, attenuation increases approximately proportionally to the sand content as seen in Fig. 10(b), a behavior typical of single scattering mechanisms [23].
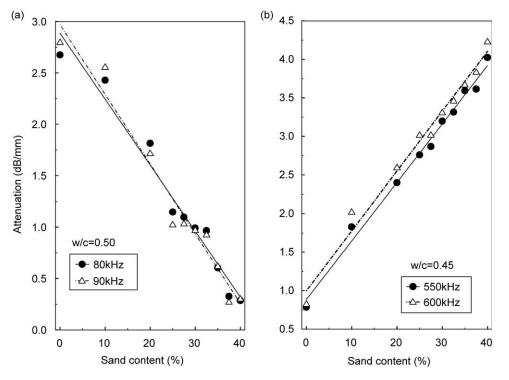

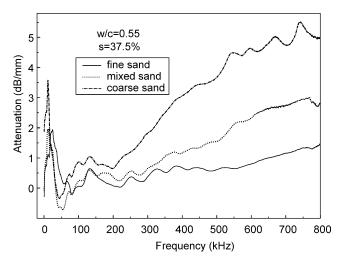Fig. 10. Attenuation vs sand content for (a) low and (b) high frequencies.

Fig. 11. Sand grain size effect on frequency dependent attenuation.

The content, however, is not the only influence of sand in attenuation. The size of the grains seems also very important. Using a simple sieve, separation of the sand in two parts was performed. The one part contained grain sizes smaller than 1 mm while the other larger than 1 mm. In Fig. 11 the difference in attenuation of specimens sharing the same s and w/c but made with different sand parts can be seen. The mortar made with the coarse sand exhibits much greater attenuation than mortar with fine sand for most frequency bands especially the high ones. This is a strong, at least, indication that scattering dominates the attenuative behavior. Also the attenuation of a mortar specimen made with unseparated sand, containing both small and larger

grains falls in between the other two curves, for most frequencies. It should be noted that throughout the whole investigation, coarse sand was used in order to lead to more pronounced and clear effects.

4.2. w/c Effect

The case concerning water content influence on attenuation is not much different from the dispersion one. Indeed w/c variation seems not to have a strong effect on attenuation of mortar. In Fig. 12(a) the attenuation vs frequency curves of different w/c specimens is depicted. Attenuation does not seem to be affected much by the w/c since all 30% by sand volume content specimens exhibit more or less the same curves. Similar are the conclusions for the case of specimens with $s = 40\%$ (Fig. 12(b)). Only for a band of frequencies around 500 kHz in these two cases it can be suggested that lower w/c ratio results in lower attenuation although this trend is not reliable since it is not repeatable for all the cases examined.

Geometric attenuation, attributed to the spreading of the wavefront over a wider volume, has always the same effect as fresh mortar specimens, used for amplitude observation, are all of the same dimensions. Concerning the material itself, as modeled in Ref. [24], in the hardened state, the attenuation behavior seems to be a function of porosity and aggregate size, being also proportional to frequency. In the present case, however, the attenuation vs frequency curve is far from being linear, making the derivation of such an empirical model troublesome. However, as seen above,
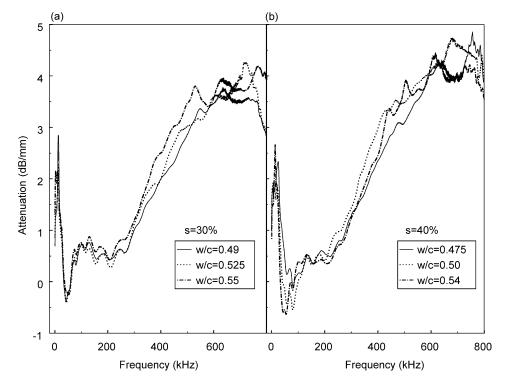

Fig. 12. Effect of w/c ratio on attenuation vs frequency curves of (a) $s = 30\%$ and (b) $s = 40\%$ specimens.
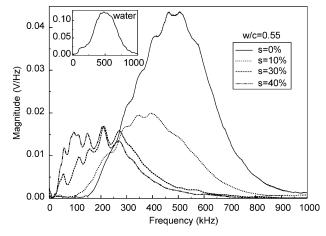
Fig. 13. FFT of sine-sweep pulses from mortar specimens with different sand content.

fresh mortar attenuation is strongly influenced by similar parameters as the sand grain size, content and frequency, while entrapped air bubbles seem to contribute to lower frequencies. A theoretical investigation is currently under way, based mainly on scattering theory [25], to examine in a comprehensive manner the complicated propagation behavior in such a medium. Nevertheless, the density of the medium, which is mainly controlled by the *w/c*, does not exercise significant influence on wave propagation parameters. The above suggest that characterization concerning sand content could be feasible. However, the estimation of *w/c*, which is a more important parameter to be determined remains troublesome since no direct effect of water content on wave parameters has been observed.

5. Sine-sweep excitation

In Section 4, the clear dependence of attenuation on sand content was described. In Fig. 13 the FFT of sine-sweep signals of mortars with different sand content is depicted. One can observe a definite shift towards the lower frequencies as *s* increases, which of course is the reason for the different calculated attenuation mentioned previously. Also, generally there exists a decrease in the overall energy. It can be said that sand acts as a cut-off filter for high frequencies (above 300 kHz) while it facilitates the propagation of lower ones (below 200 kHz). In the embedded graph of Fig. 13, the sine-sweep response of water is depicted, used for calculation of attenuation. The strong influence of sand content is obvious even from the time domain waveforms as seen in Fig. 14. There, three waveforms of materials with *w/c* = 0.55 and different *s* are depicted. It seems that the increase in sand content leads to the more rapid rise of the signal and also more rapid extinguish.

In order to draw specific information aiming at composition characterization, one should concentrate on quantifying the relationship of sand content to signal parameters that express the above mentioned frequency shift and the reinforcement of low frequency bands. After thorough examination of numerous signals, five parameters were selected. Specifically:

(i) The center frequency A_f defined as

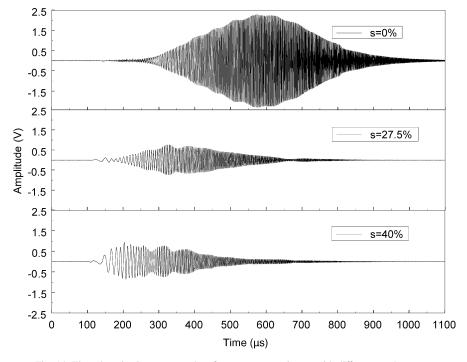$$A_f = \frac{\int fA(f)\mathrm{d}f}{\int A(f)\mathrm{d}f} \tag{3}$$

Fig. 14. Time domain sine-sweep pulses from mortar specimens with different sand content.
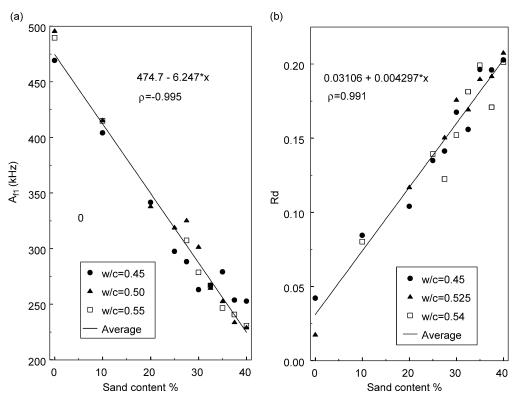
Fig. 15. Correlation plot of (a) A_{f1} vs sand content and (b) R_d vs sand content.

where f is the frequency and $A(f)$ is the spectrum of the signal.

(ii) The center frequency of the first MHz, A_{f1} focusing on the intentionally introduced frequencies, defined in a similar way.

(iii) The center time A_t

$$A_t = \frac{\int t T(t) \mathrm{d}t}{\int T(t) \mathrm{d}t} \tag{4}$$

where t is time and $T(t)$ is the rectified time signal. Finally

(iv) The ratio of the energy of the bands 130–170 kHz and
(v) 170–230 kHz to the total energy of the signal up to 1 MHz as expressed by the area under the FFT curve, henceforth denoted as R_c and R_d, respectively. All the above features exhibit strong linear correlation with s.

In Fig. 15(a) the correlation of A_{f1} with sand content is depicted clearly. It seems that irrespective of the w/c of the specimens, the center frequency follows the same decreasing trend with sand content. Similar is the case for Fig. 15(b) where the R_d vs sand content curve is depicted. Therefore, as evidenced, each of these features follow a master curve which is linearly correlated with sand content either positively or negatively and independent of w/c. Indeed in Fig. 16 the same descriptors are depicted vs w/c. In both cases (a) and (b), A_{f1} and R_d, respectively, do not exhibit any correlation to w/c. This of course is in agreement with the conclusion stated above that while sand strongly influences

the wave propagation in mortar, water content seems to be of secondary importance.

6. Material characterization

6.1. Sand content determination

Making use of the simple linear relationships between signal features and sand content and considering the high correlation coefficient of the graphs, the analysis of a signal and calculation of the selected parameters was assumed to lead to reliable sand content estimation. The above relations were obtained using responses of the first 40 specimens tested. In order to test the characterization efficiency of these descriptors in this initial stage, a number of other specimens were tested, specifically 23, and the following procedure was used.

For each specimen, three sine-sweep pulses were recorded to increase the population data after stirring each time the mortar with the stick. Calculating the above mentioned five features for each signal and through their linear relationship with s, the sand content was estimated. Therefore, 15 values of s for each specimen were obtained. From the total of 15 values, those located more than a standard deviation away from the average were considered outliers. The rest after averaging yield the predicted sand content. However, thorough investigation revealed that, for the data population of this study, the average error was decreased by excluding the two
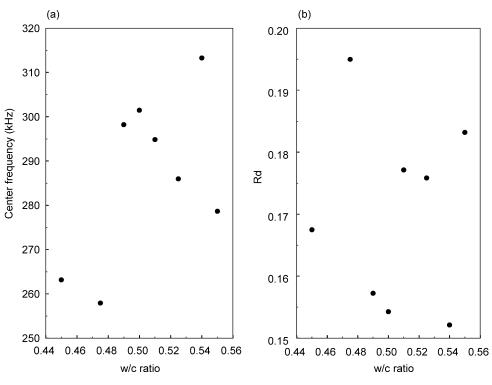
Fig. 16. Correlation plot of (a) center frequency vs *w/c* and (b) R_d vs *w/c* for specimens containing 30% sand.

minimum and two maximum values of *s*, regardless of their location with respect to the average of 15. Therefore, in this work, the predicted sand content for a specimen was taken as the average of the 11 median values of *s*, individually produced by the calculation of selected parameters of the three signals. In Fig. 17, one can observe the correlation between the predicted and actual values using the above methodology. The discrepancies are not great leading to an average error of 3.69% of absolute value, meaning, for example, that an actual volume content of 30% would be typically predicted as 31.109 or 28.891%. The above accuracy could be characterized satisfactory concerning sand content estimation.

6.2. w/c estimation

Since, as seen previously, no direct strong relation of any wave parameter with *w/c* has been observed it was assumed that water content could be calculated using the knowledge of the amount of other ingredients in mortar. Indeed, using the value of sand content obtained above and given the aggregate to cement ratio by mass, *a/c*, which is a mix design parameter supplied by the manufacturer, the water content and the *w/c* can be derived. The following relation can be easily obtained considering the sand content as the sand volume divided by the sum of volumes of all ingredients, expressing the volumes through density and mass and dividing by the cement mass, *c*

$$\frac{w}{c} = \frac{a}{c\rho_a}\left(\frac{1}{s} - 1\right) - \frac{1}{\rho_c} \qquad (5)$$

The densities of the ingredients are known in any case; values used in the calculation of this section: $\rho_a = 2.69$ g/cm^3 (sand) and $\rho_c = 3.15$ g/cm^3 (cement). The density of water was assumed to be 1 g/cm^3. Using relation (5), *w/c* values for the test specimens were calculated. Table 2 contains the results with the exception of a few cases for which the reliability of the signal was questioned.

It is seen that half of the test specimens' *w/c* is predicted with an error of 5% or less. However, there are also many cases exhibiting higher errors, even 20%, increasing the mean error of *w/c* estimation to 7.57%. Compression tests on standard mortar specimens conducted earlier in
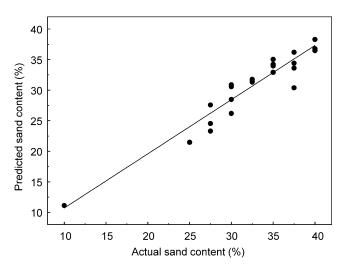

Fig. 17. Correlation plot of predicted vs actual values of sand content.

Table 2
Results of *w/c* prediction methodology

Predicted *w/c*	Actual *w/c*	Error (%)
0.541	0.54	0.22
0.524	0.54	3.03
0.625	0.54	15.77
0.510	0.49	4.17
0.480	0.49	1.98
0.523	0.49	6.81
0.491	0.49	0.17
0.558	0.49	13.78
0.604	0.51	18.41
0.449	0.51	12.01
0.495	0.51	2.87
0.504	0.51	1.19
0.580	0.51	13.65
0.522	0.51	2.39
0.482	0.525	8.14
0.450	0.525	14.21
0.527	0.525	0.45
0.463	0.475	2.52
0.433	0.475	8.92
0.574	0.475	20.76
Mean error (%)		7.57

the framework of a national project [26] revealed a decrease of 28 days strength from approximately 47 to 35 MPa for a *w/c* increase from 0.50 to 0.65. Bearing the above in mind, it can be assumed that the observed error, corresponding to 0.038 in terms of *w/c* has an impact of about 3 MPa in estimated compressive strength or approximately 7%. In practice, a deviation of 0.03 in *w/c* in certain cases would lead to further concerns about the integrity of the structure [6] while currently evaluated methods do not yield typical error less than 0.037 [9]. Therefore, the above methodology, although encouraging, needs further improvement to obtain engineering importance.

A certain concern is the entrapped air voids whose volume was excluded from the calculation relation although it actually alters the ingredients content in the specimen with respect to the designed values. This is certainly a disadvantage responsible for an amount of error, since the error of *w/c* prediction can be reduced to zero by introducing a specific air content for each specimen in (5). This was done in order to evaluate the contribution of air content in the accuracy of the methodology. The value of the air content needed to correct the *w/c* prediction for each specimen averages around 7%, which is typical for fresh mortar. However, as to the methodology, it is assumed that applying sufficient compaction the void content would be minimized and predictions of *w/c* would be more accurate. An alternative would be the use of commercial fresh concrete air content meters in order to improve accuracy. Another concern is about the accuracy of the given by the manufacturer value of *a/c*. Anyway, the evaluation of accuracy of any *w/c* determination methodology is based on comparison between experimentally obtained values with

given batch reports. The effect of these concerns should be tested and evaluated in practice.

7. Conclusions

The objective of this paper is two-fold: the study of wave propagation in fresh mortar followed by an investigation on the possibility of quality estimation through composition control. Results from the tone-burst and sine-sweep experiments indicated the dispersive and attenuative nature of fresh cementitious material. The dominant role of the inclusion (sand) content in wave propagation affecting both velocity and attenuation was highlighted. However, the contribution of other sources of inhomogeneity as the entrapped air bubbles, always present in fresh mortar, should not be neglected, since paste specimens containing no aggregates exhibit strong attenuation at low frequencies. Remarkable differences, especially in attenuation, are observed where sand rich mixes exhibit much higher attenuation than paste for frequencies above 300 kHz, while the situation is reversed for frequencies lower than 200 kHz. Also the larger grain size results in higher attenuation than fine sand leading to the assumption that scattering is the dominant attenuation mechanism. The effect of water content was not clearly observed; however, a methodology based on the determination of sand content allows for estimates of *w/c* with encouraging accuracy. The use of a more sophisticated pattern recognition approach has the potential to improve the results while theoretical investigation using multiple scattering theory, currently undertaken, could lead to an understanding of the exhibited complicated behavior.

Testing of fresh mortar is a step towards concrete examination. The practical advantage of mortar is the low volume of material required. In order to test concrete, where the maximum aggregate size is of the order of 40 mm, the experimental set-up should be drastically modified both in geometry, to contain an indicative volume of the material and probably in equipment to compensate for the reduced amplitude of the wave after several centimeters of propagation through concrete. However, considering the difficulties of ultrasound measurements in fresh concrete [1] another alternative can be examined; the assessment of mortar sieved from the given concrete. This procedure is described in the ASTM codes for measuring the setting time of concrete.

References

[1] Popovics S, Popovics JS. Ultrasonic testing to determine water–cement ratio for freshly mixed concrete. Cem Concr Aggr 1998;20(2): 262–8.

[2] Mather B. How soon is soon enough? ACI J 1976;73(3):147–50.

[3] Neville AM. Properties of concrete. London: Longman; 1995.

[4] Whiting D, Nagi M. Laboratory evaluation of nuclear gage for measurement of water and cement content of fresh concrete. ACI Mater J 1999;96(1):101–8.

[5] Mubarak K, Bois KJ, Zoughi R. A simple, robust, and on-site microwave technique for determining water-to-cement ratio (*w/c*) of fresh Portland cement-based materials. IEEE Trans Instrum Meas 2001;50(5):1255–63.

[6] Nantung TE. Determination of water-to-cement ratio in fresh concrete using microwave oven, evaluation of SHRP product. Indiana Department of Transportation; 1998.

[7] Grosse CU, Reinhardt HW. Continuous ultrasound measurement during setting and hardening of concrete. Otto Graf J 1994;5:76–98.

[8] Naik TR, Ramme BW. Determination of the water–cement ratio of concrete by the buoyancy principle. ACI Mater J 1989;86(1):3–9.

[9] Dowell A, Cramer S. Field measurement of water–cement ratio, final report. Wisconsin Highway Research Program #0092-45-16, Wisconsin Department of Transportation; 2002.

[10] Kaplan MF. The effects of age and water/cement ratio upon the relation between ultrasonic pulse velocity and compressive strength. Mag Con Res 1959;11(32):85–92.

[11] Valic MI. Hydration of cementitious materials by pulse echo USWR method, apparatus and application examples. Cem Concr Res 2000; 30:1633–40.

[12] Boumiz A, Vernet C, Cohen Tenoudji F. Mechanical properties of cement pastes and mortars at early ages. Adv Cem Based Mater 1996; 3:94–106.

[13] Reinhardt HV, Grosse CU, Herb AT. Ultrasonic monitoring of setting and hardening of cement mortar—a new device. Mater Struct 2000; 33:580–3.

[14] Chotard T, Gimet-Breart N, Smith A, Fargeot D, Bonnet JP, Gault C. Application of ultrasonic testing to describe the hydration of calcium aluminate cement at the early age. Cem Concr Res 2001;31:405–12.

[15] Grosse CU, Reinhardt HW. Fresh concrete monitored by ultrasound methods. Otto Graf J 2001;12:157–68.

[16] Arnaud L, Thinet S. Mechanical evolution of concrete during setting. Mater Struct 2003;36:355–64.

[17] Akkaya Y, Voigt T, Subramaniam KV, Shah S. Nondestructive measurement of concrete strength gain by an ultrasonic wave reflection method. Mater Struct 2003;36:507–14.

[18] Harker AH, Temple JAG. Velocity and attenuation of ultrasound in suspensions of particles in fluids. J Phys D: Appl Phys 1988;21: 1576–88.

[19] Allegra JR, Hawley SA. Attenuation of sound in suspensions and emulsions: theory and experiments. J Acoust Soc Am 1972;51(5): 1545–64.

[20] Philippidis TP, Aggelis DG. An acousto-ultrasonic approach for the determination of water to cement ratio in concrete. Cem Concr Res 2003;33(4):525–38.

[21] Fowler KA, Elfbaum GM, Smith KA, Nelligan TJ. Theory and application of precision ultrasonic thickness gaging. NDTnet 1997; 10(2).

[22] McClements DJ. Ultrasonic measurements in particle size analysis. In: Meyers RA, editor. Encyclopedia of analytical chemistry. Chichester: Wiley; 2000.

[23] Farrow CA, Anson LW, Chivers RC. Multiple scattering of ultrasound in suspensions. Acustica 1995;81:402–11.

[24] Schickert M. Ultrasonics NDE of concrete. In: 2002 IEEE Ultrasonics Symposium, New York: IEEE; 2002. p. 739–48.

[25] Foldy LL. The multiple scattering of waves. Phys Rev 1945;67(3): 107–19.

[26] Aggelis DG, Polyzos D, Philippidis TP, Tsimogiannis A, Anastasopoulos A, Georgali B, Kaloidas B. Non destructive estimation of mortar's composition and strength using acousto-ultrasonics. In: Proceedings of the First Hellenic Conference on Concrete Composite Materials, Xanthi; 2000. p. 49–71 [in Greek].